Electronic Supplementary Material (ESI) for Physical Chemistry Chemical Physics.

Electronic Supporting Information

Understanding the effects of targeted modifications on the 1:2 Choline And GEranate structure

Ana Dobre,[‡,a] Spyridon Koutsoukos,[‡,a,b] Frederik Philippi,[a] Daniel Rauber,[c] Christopher W. M. Kay,[c,d] Oriele Palumbo,[e] Maxie M. Roessler[a,b] and Tom Welton [*,a]

[a.] *Department of Chemistry, Molecular Sciences Research Hub, Imperial College London, White City Campus, London W12 0BZ, UK.*
**E-mail: t.welton@imperial.ac.uk*
[b.] *Centre for Pulse EPR Spectroscopy (PEPR), Imperial College London, White City Campus, London, W12 0BZ, UK.*
[c.] *Department of Chemistry, Saarland University, Campus B2.2, Saarbrücken, Germany.*
[d.] *London Centre for Nanotechnology, University College London, 17–19 Gordon Street, London WC1H 0AH, UK.*
[e.] *Consiglio Nazionale delle Ricerche, Istituto dei Sistemi Complessi, Piazzale Aldo Moro 5, 00185 Rome, Italy.*

Table of Contents

A. Synthetic procedures

Choline bicarbonate (80 wt% aqueous), geranic acid (85% technical grade), octanoic acid, N,N-dimethylbutylamine and dimethyl carbonate were purchased from Sigma-Aldrich (Merck, Germany). TEMPO, 4-amino-TEMPO and 4-hydroxy-TEMPO were purchased from Fluorochem. 4-Carboxy-TEMPO was purchased from TCI Chemicals. 4-Oxo-TEMPO was purchased from Alfa Aesar. All chemicals were used without further purification unless stated otherwise. Choline bicarbonate was titrated prior to its use to calculate its exact concentration. Geranic acid (85% technical grade) was purified according to a modified literature procedure.[1] Briefly, the acid was crystallised from a 60 wt% geranic acid/40 wt% hexane solution at −78 °C; this procedure was repeated 4-5 times before use.

Synthesis of CAGE-derivatives

Choline and geranate (CAGE). Choline and geranate (CAGE) was synthesised according to literature.[1] Briefly, a mixture of choline bicarbonate (75 wt% in water, 10.62 g, 50.2 mmol) and ethanol (20 mL) was cooled in an ice bath to 0 °C. To this was added dropwise a solution of geranic acid (16.87 g, 100.3 mmol, 2.0 eq.) in ethanol (30 mL). The reaction mixture was allowed to warm up to room temperature and stirred for 3 h. The solvent was removed under reduced pressure and the resulting viscous oil was dried under high vacuum for 24 hours, at room temperature. CAGE was obtained as a viscous light-yellow oil (21.68 g, 49.4 mmol, 98%). ^{1}H NMR (400 MHz, DMSO-d6) δ (ppm) 1.57 (s, 6 H, Ger-CH_3), 1.64 (s, 6 H, Ger-CH_3), 1.92-2.12 (m, 14 H, Ger-C(4,5)H_2C3(CH_3)), 3.14 (s, 9 H, Ch-N(CH_3)$_3$), 3.43 (m, 2 H, Ch-C1(H_2)), 3.86 (m, 2 H, Ch-C2(H_2)), 5.08 (s, 2H, Ger-C6(H)), 5.56 (s, 2H, Ger-C2(H)); ^{13}C NMR (100 MHz, DMSO-d6) δ 18.0, 25.5, 25.8, 53.5, 55.6, 67.4, 121.6, 124.7, 131.2, 149.4, 169.4.

Choline and octanoate (CAOC). To a mixture of choline bicarbonate (80 wt% in water, 1.0 eq.) and ethanol was added dropwise a solution of octanoic acid (2.0 eq.) in ethanol. The mixture was stirred at room temperature for 3 h. The solvent was removed under reduced pressure and the resulting viscous oil was dried under high vacuum for 24 h, at room temperature. CAOC was obtained in a 92% yield as a colourless gel. 1H NMR (400 MHz, DMSO-d6) δ 0.85 (t, 6 H, J = 8.0 Hz, Oct-C8(H3)), 1.23 (m, 16 H, Oct-C(4,5,6,7)H2), 1.42 (m, 4 H, Oct-C3(H2)), 2.00 (t, 4 H, J = 8.00 Hz, Oct-C2(H2)), 3.11 (s, 9 H, Ch-N(CH3)3), 3.42 (m, 2 H, Ch-C1(H2)), 3.84 (m, 2 H, Ch-C2(H2)); 13C NMR (100 MHZ, DMSO-d6) δ 14.4, 22.1, 25.6, 28.1, 29.0, 31.3, 36.2, 53.1, 55.0, 65.6, 174.35 (CO2H and CO2−).

Butyltrimethylammonium and octanoate (BTMAAOC). Butyldimethylamine (3.07 g, 30.3 mmol, 1.0 eq), dimethyl carbonate (5.81 mL, 6.2 mmol, 2.3 equiv.) and methanol were loaded into a pressure tube, sealed and heated to 125 °C. The mixture was stirred for 18 h until ^{1}H NMR of the mixture showed complete consumption of the starting amine. The mixture was allowed to cool to room temperature, then a solution of octanoic acid (8.65 g, 60.0 mmol, 2.0 eq.) in methanol was added dropwise and the mixture was stirred at room temperature overnight. Methanol and activated charcoal (Norit SX ultra, steam-activated and acid-washed, highly purified, SIGMA-ALDRICH, St. Louis, USA) were added and the mixture was stirred at room temperature for 3 days. The charcoal was removed first by gravity filtration, then by filtering through a 0.2 µm PTFE membrane and finally by passing the mixture through a C18 reverse phase column. The solvent was removed under reduced pressure and the resulting viscous oil was dried under high vacuum for 24 h. BTMAAOC (10.60 g, 26.3 mmol, 87%) was obtained as a light-yellow gel that melts in the hand. 1H NMR (400 MHz, DMSO-d6) δ 0.85 (t, 6 H, J = 7.0 Hz, Oct-C8(H3)), 0.93 (t, 3 H, J = 7.3 Hz, BTMA-C4(H3)), 1.22 - 1.34 (m, 18 H, BTMA-C3(H2) & Oct-C(4,5,6,7)H2), 1.42 (m, 4 H, Oct-C3(H2)), 1.65 (m, 2 H, BTMA-C2(H2)), 1.99 (t, 4 H,

Oct-C2(H2)), 3.04 (s, 9 H, BTMA-N(CH3)3), 3.25 - 3.29 (m, 2 H, BTMA-C1(H2); 13C{1H} NMR (100 MHz, DMSO-d6) δ 13.3, 14.4, 18.3, 22.6, 24.5, 26.2, 28.5, 30.0, 31.8, 36.3, 51.8, 64.5, 176.7 (CO2H and CO2−).

Synthesis of TEMPO-derivatives

Cholinium 4-carboxylate-TEMPO ([Ch][TEMPO-COO])

To a mixture of choline bicarbonate (80 wt% in water, 1.0 eq.) and ethanol, a solution of 4-carboxy-TEMPO (1.0 eq.) in ethanol was added. The mixture was stirred at room temperature under nitrogen atmosphere for 3 h. The solvent was removed under reduced pressure and the resulting viscous oil was dried under high vacuum for 24 h. [Ch][TEMPO-COO] was obtained in a 100% yield as an orange solid. ^{1}H NMR (400 MHz, D_2O with one drop of phenylhydrazine) δ (ppm): 3.11 (s, 9H, choline-N(Me)$_3$), 2.12-2.01 (tt, 1H, OOC-TEMPO-C4(H)), 1.6-1.52 (m, 4H, OOC-TEMPO-C(2,5)H$_2$),1.35-1.26 (m, 4H, OOC-TEMPO-C(2,5)H$_2$), 1.01 & 0.96 (s & s, 9H, OOC-TEMPO-C(2,5)-(Me)$_4$). ES$^+$: 103.8 (M+, 100%); ES$^-$: 199.1 (M-, 100%).

Butyldimethylammonium 4-carboxylate-TEMPO ([BTMA][TEMPO-COO])

Butyldimethylamine (1.0 eq.), dimethyl carbonate (2.3 eq.) and methanol were loaded into a pressure tube (Ace Glass), sealed with a silicone o-ring and heated to 125 °C. The mixture was stirred for 18 h until ^{1}H NMR of the mixture showed complete consumption of the starting amine. The mixture was allowed to cool to room temperature, then a solution of 4-carboxy-TEMPO (1.0 eq.) in methanol was added dropwise and the mixture was stirred at room temperature overnight. Methanol and activated charcoal (Norit SX ultra, steam activated and acid washed, highly purified, SIGMA-ALDRICH, St. Louis, USA) were added and the mixture was stirred at room temperature for 3 days. The charcoal was removed first by gravity filtration, then by filtering through a 0.2 µm PTFE membrane and finally by passing the mixture through a C18 reversed phase chromatography column. The solvent was removed under reduced pressure and the resulting waxy product was dried under high vacuum for 24 h. [BTMA][TEMPO-COO] was obtained in 85% yield as an orange wax. ^{1}H NMR (400 MHz, DMSO-d6 with one drop of phenylhydrazine) δ (ppm): 3.30-3.22 (m, 2H, BTMA-C(1)H$_2$), 3.04 (s, 9H, BTMA-N(Me)$_3$), 2.29-2.21 (tt, 1H, OOC-TEMPO-C4(H)), 1.7-1.54 (m, 4H, OOC-TEMPO-C(2,5)H$_2$), 1.38-1.24 (m, 4H, BTMA-C(2,3)H$_2$), 1.02 & 0.97 (s & s, 9H, OOC-TEMPO-C(2,5)(Me)$_4$), 0.93 (t, 3H, BTMA-C(4)H$_3$). ES$^+$: 116.1 (M+, 100%); ES$^-$: 199.1 (M-, 100%).

Trimethylammonium-TEMPO iodide ([TMA-TEMPO]I)

[TMA-TEMPO]I was synthesised according to the procedure by Luo *et al.*[2] with slight modifications. Briefly, 1.0 eq. of 2,2,6,6-Tetramethyloxy-4-aminopiperidine (2 g, 11.7 mmol) was dissolved in 20 mL of acetone and mixed with 6.0 eq. of methyl iodide (10.2 g, 70.2 mmol). The solution was stirred at room temperature for 5 h until a light orange precipitate was formed. The precipitate was filtered and washed 3 times with 5 mL of cold acetone, in order to purify it from the residual starting materials. Light orange powder was collected (37% yield, 1.4 g, 4.3 mmol). ^{1}H NMR (400 MHz, D_2O with one drop of phenylhydrazine) δ (ppm): 3.64-3.54 (m, 1H, TMA-TEMPO-C(4)H), 2.96 (s, 9H, TEMPO-N(Me)$_3$), 2.06 & 1.62 (d & t, 4H, TMA-TEMPO C(2,5)H$_2$), 1.13 & 1.09 (s & s, 9H, TMA-TEMPO-C(2,5)(Me)$_4$). ES$^+$: 241.2 (M+, 100%); ES-: 126.9 (M-, 100%), 380.6 (M$_3^-$, 45%).

Trimethylammonium-TEMPO octanoate ([TMA-TEMPO][Oc])

A concentrated aqueous solution of [TMA-TEMPO]I containing a small amount of THF (for solubility purposes) was passed through a chromatography column packed with Amberlyst A-27 anion exchange resin to obtain

the cation with hydroxide anion. The aqueous solution was neutralised with 1 eq. octanoic acid in ethanol. The solvent was removed under reduced pressure and the resulting orange product was dried under high vacuum for 24 h, at room temperature. [TMA-TEMPO][Oc] was obtained in a 100% yield as an orange wax. ^{1}H NMR (400 MHz, D_2O with one drop of phenylhydrazine) δ (ppm): 3.77-3.64 (m, 1H, TMA-TEMPO-C4(H)), 2.96 (s, 9H, TEMPO-N(Me)$_3$), 2.00 & 1.92 (d & t, 4H, TMA-TEMPOC(2,5)H_2), 1.31 - 0.98 (m, 21H, TMA-TEMPO-C(2,5)(Me)$_4$ and Oc-C(2-7)H_2), 0.86 (t, 3H, Oc-C(1)H_3). ES^+: 214.2 (M+, 100%); ES^-: 143.1 (M-, 100%).

Trimethylammonium-TEMPO geranate ([TMA-TEMPO][Ge])

A concentrated aqueous solution of [TMA-TEMPO]I containing a small amount of THF (for solubility purposes) was passed through a chromatography column packed with Amberlyst A-27 anion exchange resin to obtain the cation with hydroxide anion. The aqueous solution was neutralised with 1 eq. purified geranic acid in ethanol. The solvent was removed under reduced pressure and the resulting orange product was dried under high vacuum for 24 h, at room temperature. [TMA-TEMPO][Ge] was obtained in a 100% yield as an orange viscous liquid. ^{1}H NMR (400 MHz, DMSO-d_6 with one drop of pentafluophenylhydrazine) δ 5.48 (s, 1H, Ge-C(2)H), 5.07 (m, 1H, Ge-C(6)H), 3.74–3.64 (m, 1H, TMA-TEMPO-C4(H)), 3.01 (s, 9H, TEMPO-N(Me)$_3$), 2.09–1.91 (m, 9H, TMA-TEMPO C(3,5)H_2 and Ge-C(3',4,5), 1.67–1.52 (m, 8H, TMA-TEMPO (C3,5)H_2 and Ge-C(8,8')H_3), 1.16–1.03 (m, 12H, TMA-TEMPO-C(2,6)(Me)$_4$); ES^+: 214.2 (M+, 100%), ES^-: 167.1 (M-, 100%).

B. Thermal Transitions

Thermal transitions measured via DSC are given in Table S1. The enthalpy of fusion (associated with the sample melting) and the enthalpy of the endothermic liquid-liquid phase transition are calculated as the area under the curve. The entropy is calculated as the enthalpy divided by the transition temperature in Kelvin.

Table S1. DSC data for the studied DESs

DES	T_g / °C	T_c / °C	T_m / °C	ΔH_{fus} / kJ mol^{-1}	ΔS_m / J mol^{-1} K^{-1}	$T_{l\text{-}l}$ / °C	$\Delta H_{l\text{-}l}$ / kJ mol^{-1}	$\Delta S_{l\text{-}l}$ / J mol^{-1} K^{-1}
CAGE	− 83	−14	−10	0.37 ± 0.01	1.40 ± 0.02	--	--	--
CAOC	− 95	−35[a]	−28	1.37 ± 0.04	5.57 ± 0.15	52	1.20 ± 0.01	3.69 ± 0.03
BTMAAOC	− 95	−34[a]	−20	2.59 ± 0.18	10.24 ± 0.69	17	1.62 ± 0.03	5.59 ± 0.10

[a] Cold crystallisation

C. Viscosities

Dynamic viscosity measurements were performed for CAGE in the range 298.15 – 378.15 K. For BTMAAOC and CAOC dynamic viscosity was measured only in the isotropic region: 318.15 – 378.15 K for BTMAAOC and 318.15 – 378.15 K for CAOC. The experimental data were fitted using the Vogel-Fulcher-Tammann equation:

$$\eta = \eta_0 \cdot e^{\frac{B}{T-T_0}} \quad \text{(S1)}$$

with η_0, B and T_0 being empirical fitting parameters.

The fit parameters η_0, B and T_o are given in Table S2.

Table S2. Experimental viscosities of the studied ILs. The deviation δ is calculated according to Equation S2 and is relative to the fitting data.

T / K	CAGE		BTMAAOC		CAOC	
	η / mPa s	δ / %	η / mPa s	δ / %	η / mPa s	δ / %
298.15	1134.25	0.05	--	--	--	--
303.15	801.84	−0.2	--	--	--	--
308.15	583.83	0.1	--	--	--	--
313.15	433.34	0.2	--	--	--	--
318.15	327.11	0.06	150.30	−0.004	--	--
323.15	251.19	−0.1	115.83	−0.005	--	--
328.15	196.42	−0.1	90.82	0.04	177.89	0.07
333.15	156.08	0.06	72.14	−0.1	141.66	−0.2
338.15	125.15	−0.2	58.28	0.001	114.89	0.1
343.15	101.86	−0.2	47.70	0.2	94.21	0.5
348.15	83.87	−0.08	39.35	−0.02	77.29	−0.1
353.15	69.74	−0.06	32.86	−0.05	64.25	−0.3
358.15	58.61	0.08	27.73	0.004	54.03	−0.2
363.15	49.59	0.02	23.60	−0.008	45.89	0.04
368.15	42.37	0.1	20.25	−0.003	39.15	0.02
373.15	36.45	0.1	17.51	−0.02	33.64	−0.007
378.15	31.52	−0.01	15.24	−0.07	29.22	0.4

The relative deviation of the viscosity (δ) with respect to the fitting data was calculated using Equation S2:

$$\delta = \frac{100(\eta_{\text{exp}} - \eta_{\text{calc}})}{\eta_{\text{calc}}} \quad \text{(S2)}$$

The absolute average deviation (AAD%) between the measured and fitted data was calculated using Equation S3:

$$AAD = \frac{100}{N} \sum_{i=1}^{N} \left(\frac{|\eta_{exp_i} - \eta_{calc_i}|}{\eta_{exp_i}} \right) \quad \text{(S3)}$$

(S3)

In both equations, η_{exp} represents experimental values and η_{calc} represents calculated values obtained from the fitting of viscosity against temperature according to Equation S1.

Table S3. Parameters η_0, B and T_0 from the Vogel-Fulcher-Tammann equation used to fit the experimental viscosities as a function of temperature, and the absolute average deviation (AAD).

Sample	η_0 / mPa s	B / K	B / kJ mol^{-1}	T_0 / K	AAD / %
CAGE	0.0766	1290.87	10.73	163.72	0.004
BTMAAOC	0.0601	1135.71	9.44	172.99	0.006
CAOC	0.0412	1517.05	12.61	146.90	0.02

Additionally, oscillating-frequency viscosity measurements were performed for CAOC (30 – 70 °C, 303.15 – 343.15 K) and BTMAAOC (25 – 55 °C, 298.15-328.15 K). The dependence of the complex viscosity (η*) on angular frequency is shown for CAOC in Figure S.1 and for BTMAAOC in Figure S.2.

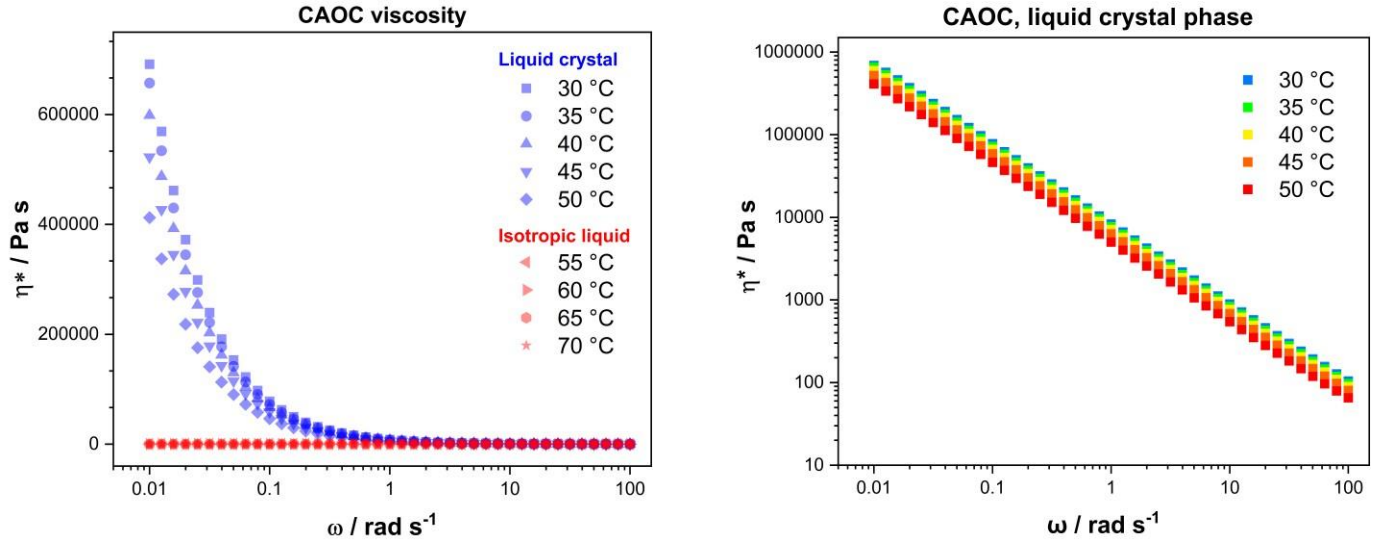

Figure S1. *Left*: complex viscosity of CAOC against angular frequency of oscillation. The blue data corresponds to the liquid-crystal phase of the system, while the red data corresponds to the isotropic liquid phase. *Right*: log-log plot of complex viscosity against angular frequency for CAOC in the liquid-crystal phase.

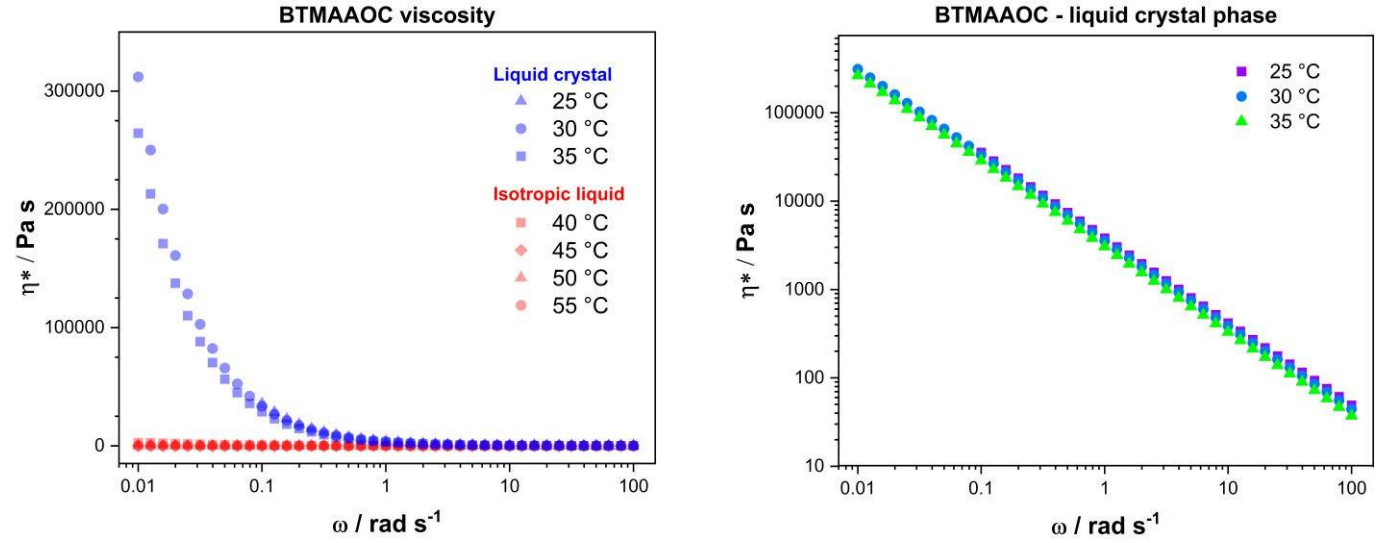

Figure S2. *Left*: complex viscosity of BTMAAOC against angular frequency of oscillation. The blue data corresponds to the liquid-crystal phase of the system, while the red data corresponds to the isotropic liquid phase. *Right*: log-log plot of complex viscosity against angular frequency for BTMAAOC in the liquid-crystal phase.

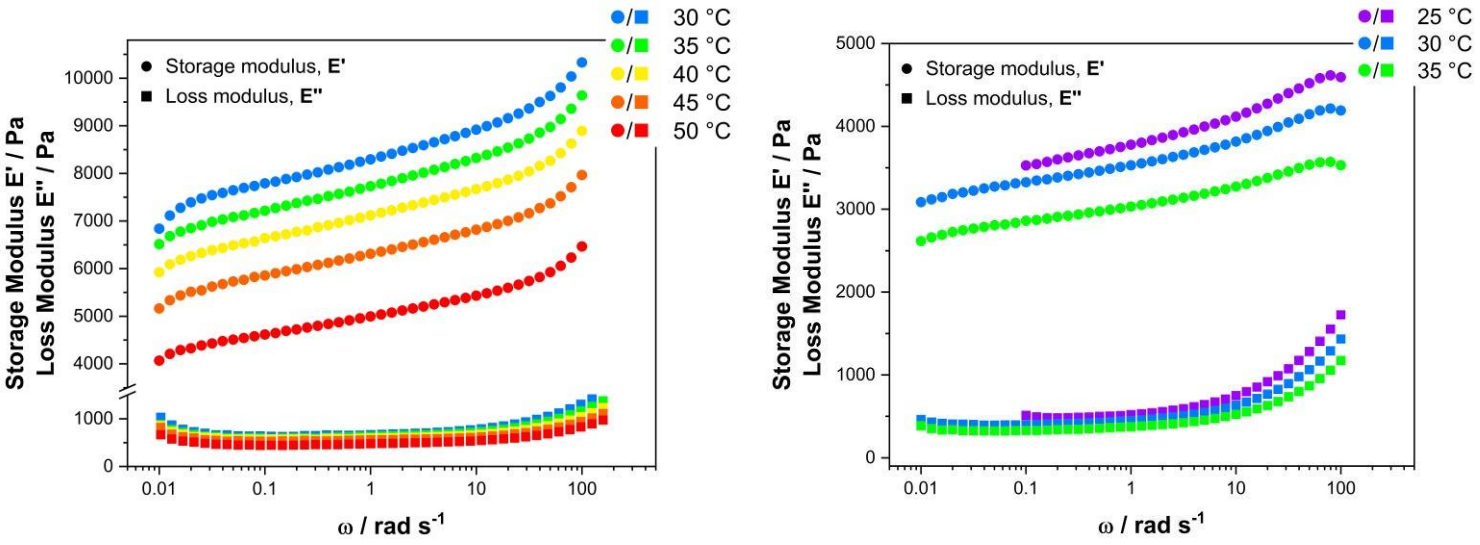

Figure S3. Storage modulus (*E'*) and loss modulus (*E''*) of CAOC (left) and BTMAAOC (right) at temperatures below that of the liquid-liquid phase transition. *E'* is represented by circle symbols and *E''* by squares.

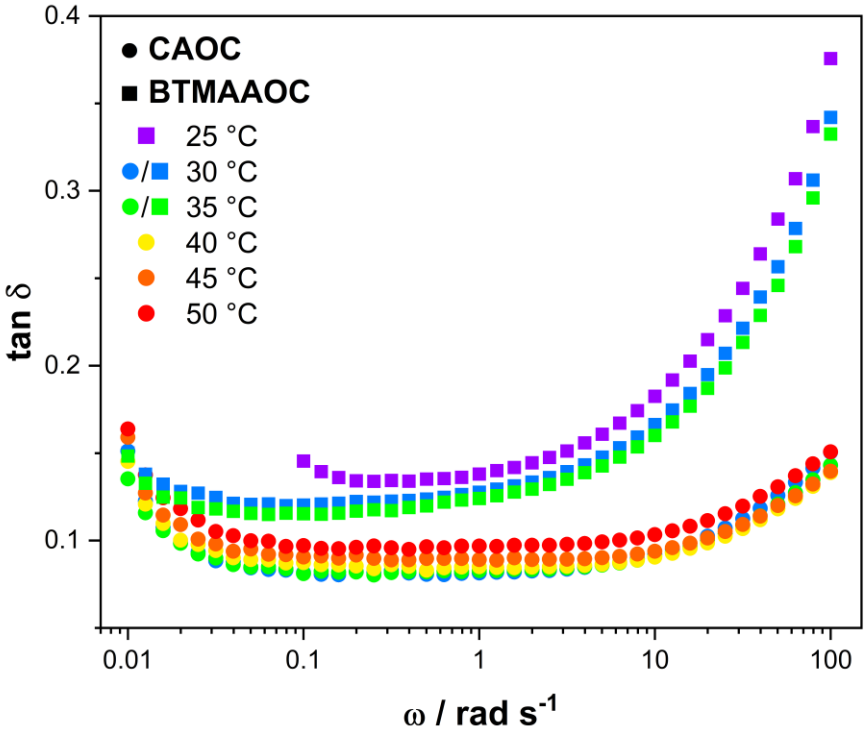

Figure S4. Loss tangent (tan *δ*) of CAOC (circle symbols) and BTMAAOC (square symbols) at temperatures below that of the liquid-liquid phase transition

D. Dynamic Mechanical Analysis (DMA)

Table S4. Best-fit parameters τ_0, B and T_0 and α from the fitting of the thermally activated tan δ peaks in the DMA spectra

Sample	τ_0 / s	B / K	B / kJ mol^{-1}	T_0 / K	α
CAGE	(7.4±0.2) 10^{-7}	1023±14	8.5±0.1	157±3	0.79±0.02
BTMAAOC	(5.7±2.0) 10^{-7}	1076±26	8.9±0.2	169±2	0.57±0.09
CAOC	(5.5±0.1) 10^{-7}	1503±19	12.5±0.2	134±2	0.75±0.01

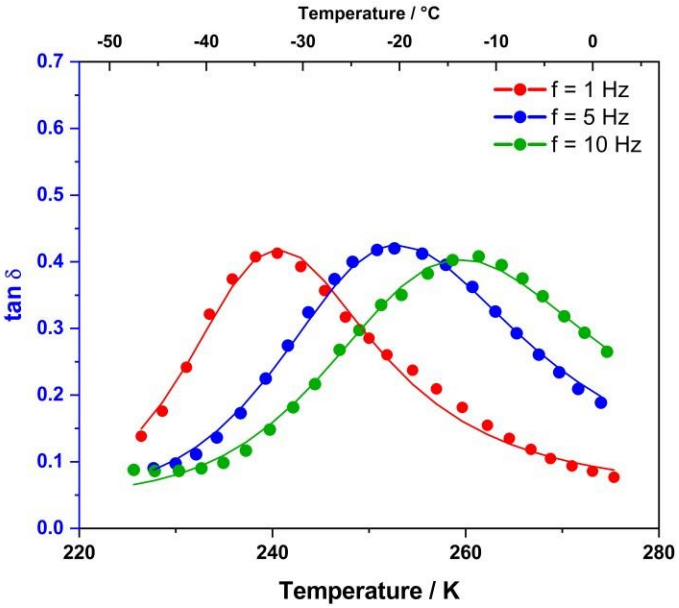

Figure S5. Loss tangent (tan δ) of CAGE measured on cooling at f = 1, 5 and 10 Hz. Only the peak corresponding to the thermally activated relaxation is shown. The solid lines are the result of a global fit across all three frequencies. Before fitting, a background subtraction was performed. Only the data that was not affected by the presence of a shoulder peak at high temperatures was included in the fit.

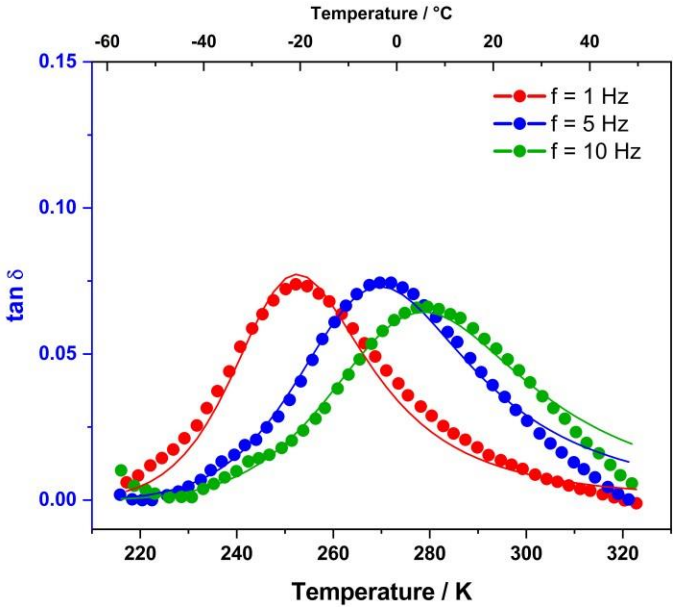

Figure S6. Loss tangent (tan δ) of CAOC measured on cooling at f = 1, 5 and 10 Hz. Only the peak corresponding to the thermally-activated relaxation is shown. The solid lines are the result of a global fit across all three frequencies. Before fitting, a background subtraction was performed. Only the data that was not affected by the presence of a shoulder peak at high temperatures was included in the fit.

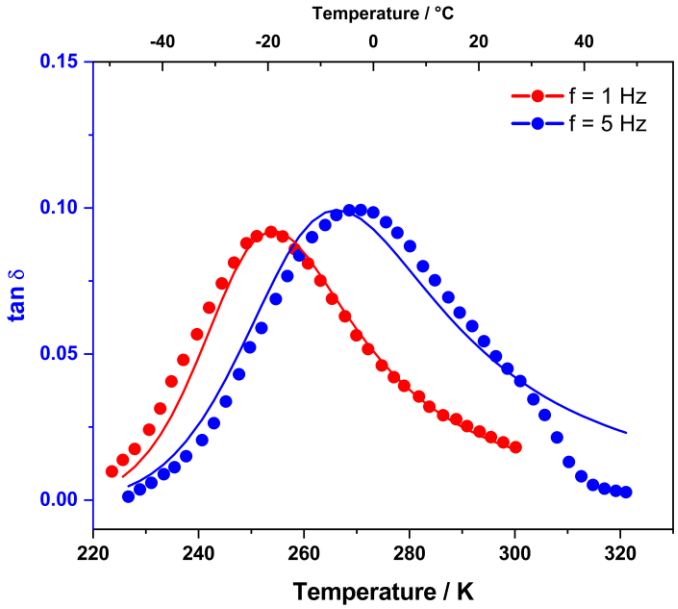

Figure S7. Loss tangent (tan δ) of BTMAAOC measured on cooling at f = 1 and 5 Hz. Only the peak corresponding to the thermally-activated relaxation is shown. The solid lines are the result of a global fit across the two frequencies. Before fitting, a background subtraction was performed. Only the data that was not affected by the presence of a shoulder peak at high temperatures was included in the fit. Data at f = 10 Hz was recorded but could not be used due to the extensive overlap between the relaxation and phase transition peaks.

E. Polarising Microscopy

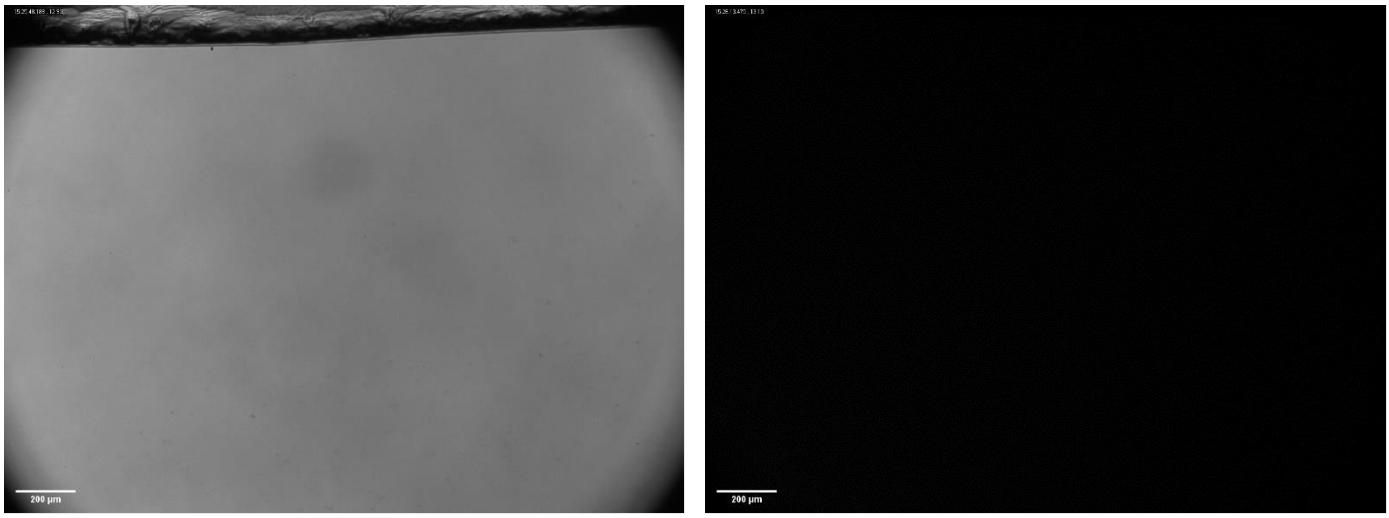

Figure S8. Microscope images of CAGE at 13 °C: brightfield (left) and polarised-light (right). The polarised-light image is entirely dark, showing that neat CAGE is not birefringent.

F. Electron Paramagnetic Resonance spectroscopy (EPR) and X-ray crystallography

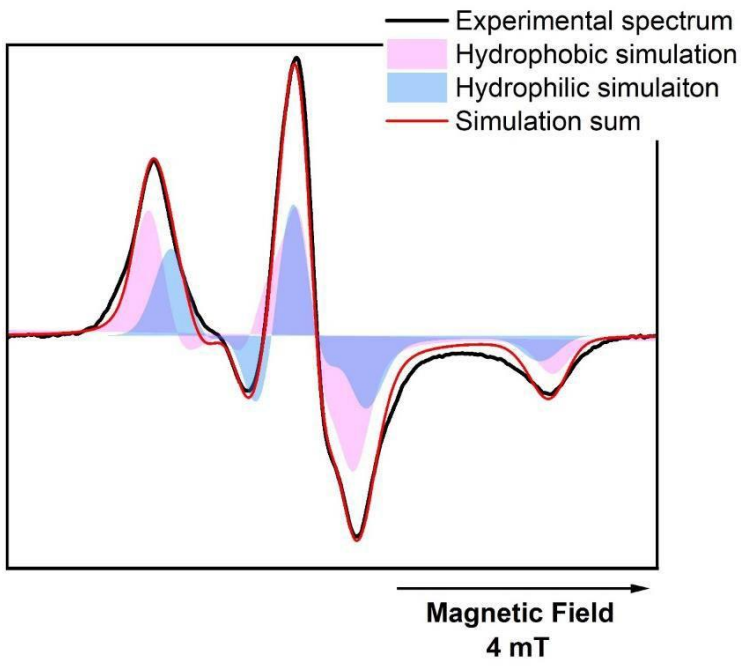

Figure S9. Experimental (black line), simulated hydrophobic domain (pink shaded), simulated hydrophilic domain (blue shaded) and simulation sum (red line) solid-state spectra of 1 mM 4-hydroxy-TEMPO in CAGE.

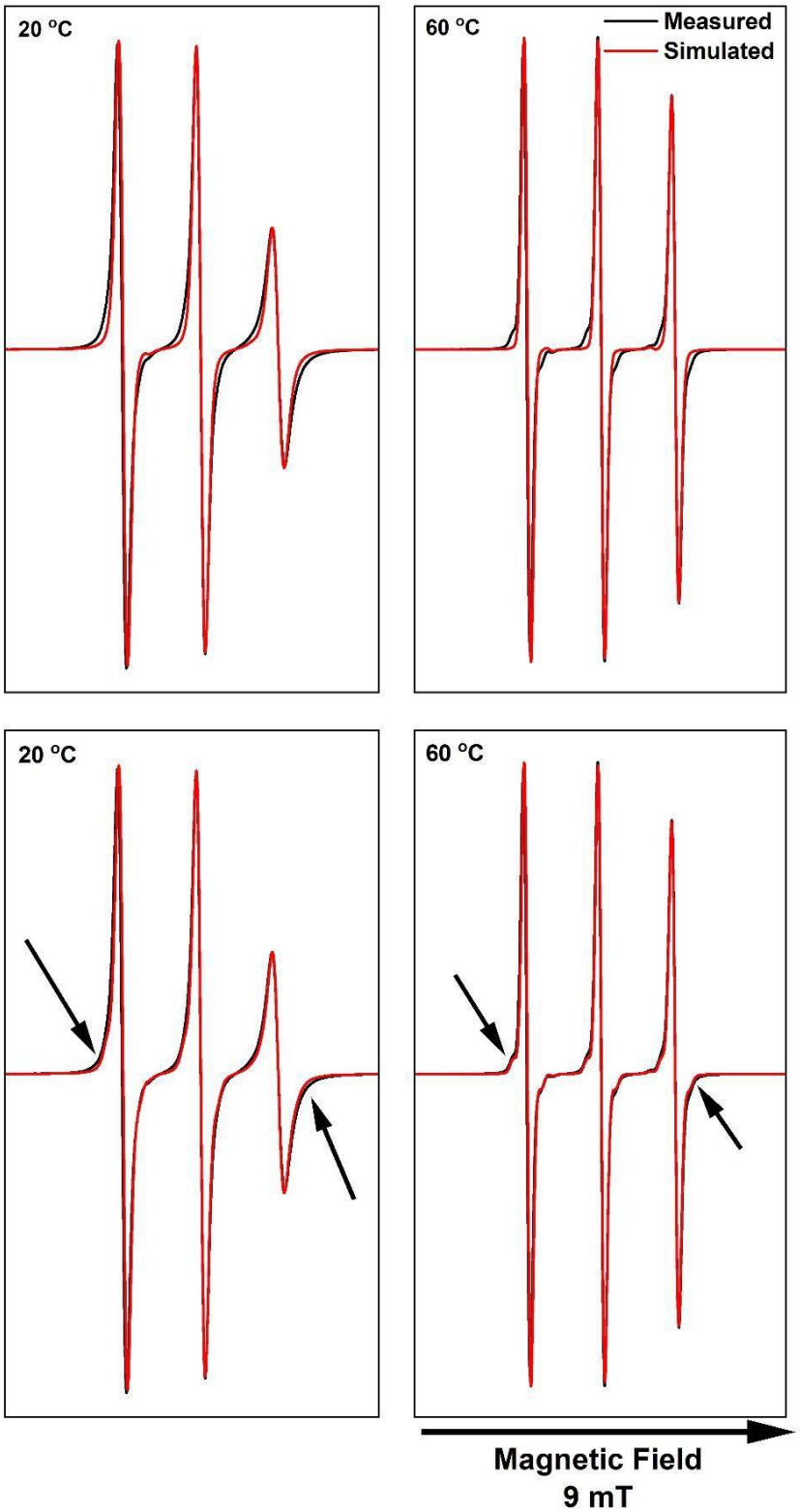

Figure S10. Measured (black) and simulated (red) X-band CW EPR spectra of 1 mM TEMPO in CAGE. The measurements were performed at 100 kHz mod. frequency and 1 mW microwave power. The top row of spectra is simulated without the addition of satellites due to ^{13}C, while the bottom row spectra have been simulated including satellites. The arrows indicate the effect of ^{13}C on the spectral shape.

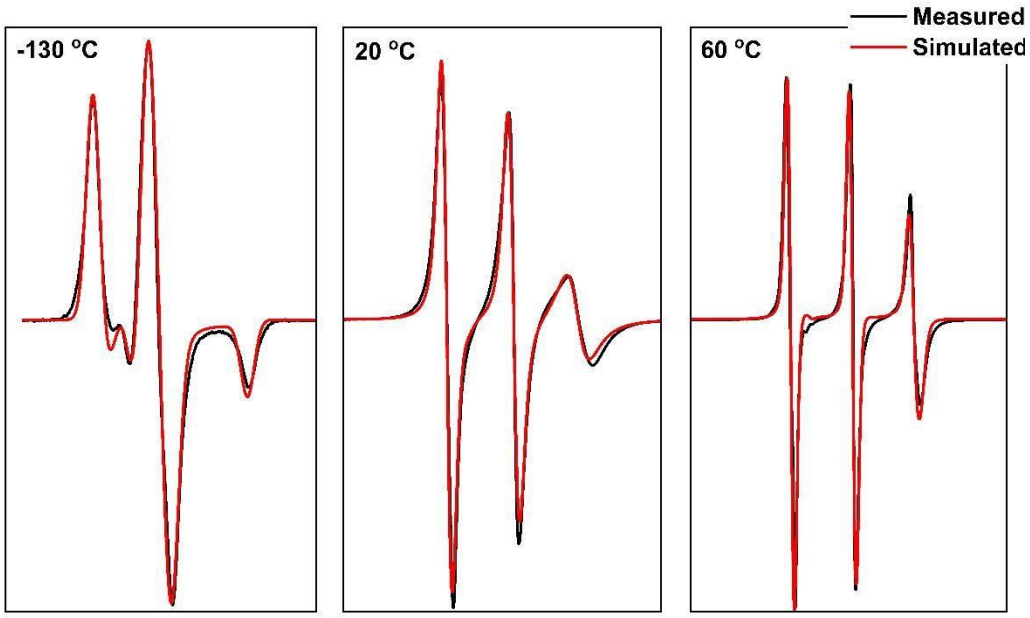

Figure S11. Measured (black) and simulated (red) X-band CW EPR spectra of 1 mM 4-hydroxy-TEMPO in CAGE. The measurements were performed at 100 kHz mod. frequency and 1 mW microwave power.

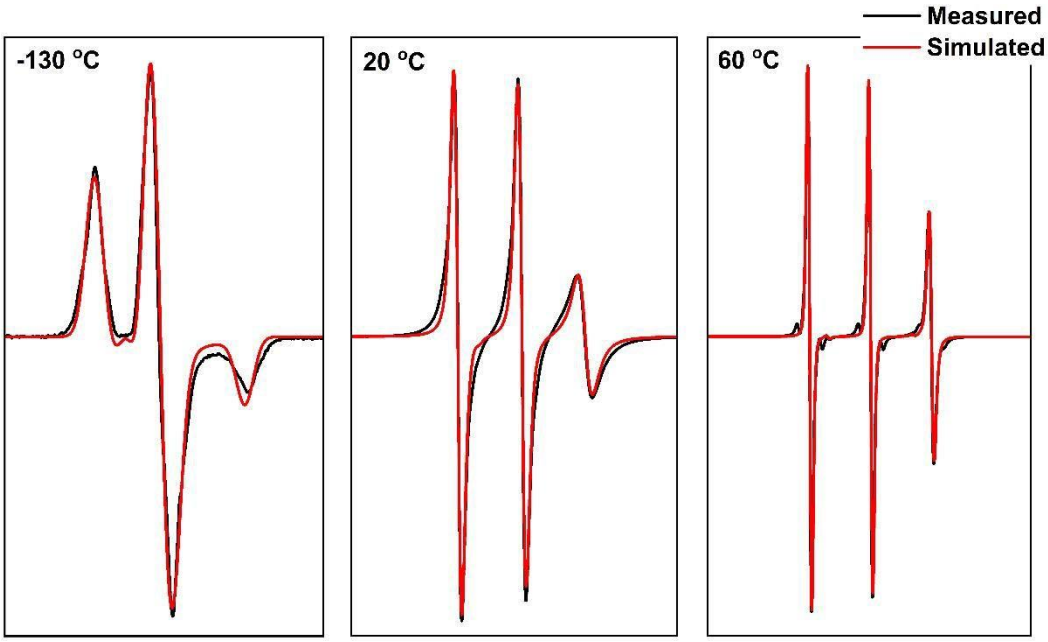

Figure S12. Measured (black) and simulated (red) X-band CW EPR spectra of 1 mM 4-oxo-TEMPO in CAGE. The measurements were performed at 100 kHz mod. frequency and 1 mW microwave power.

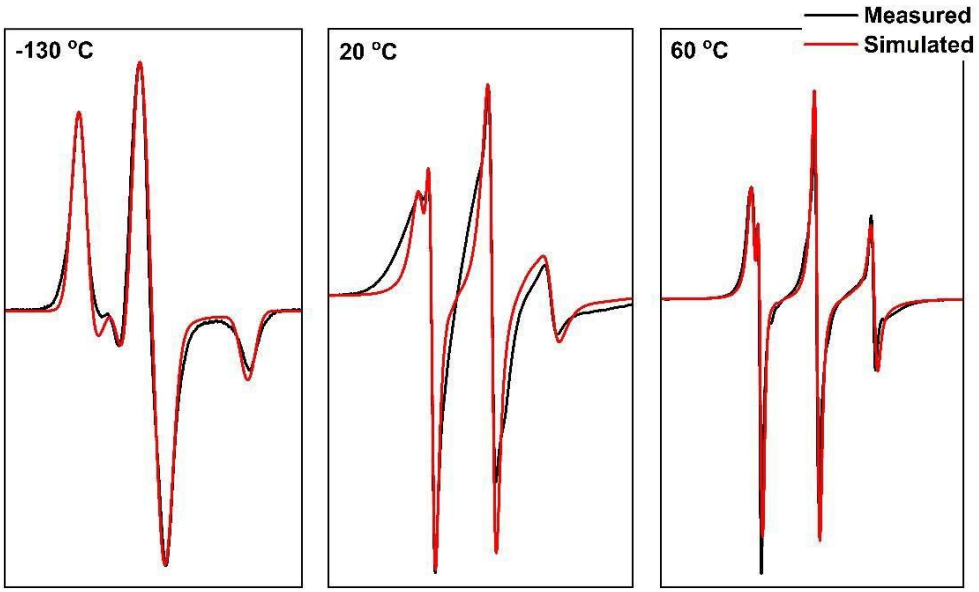

Figure S13. Measured (black) and simulated (red) X-band CW EPR spectra of 1 mM [TMA-TEMPO][Ge] in CAGE. The measurements were performed at 100 kHz mod. frequency and 1 mW microwave power.

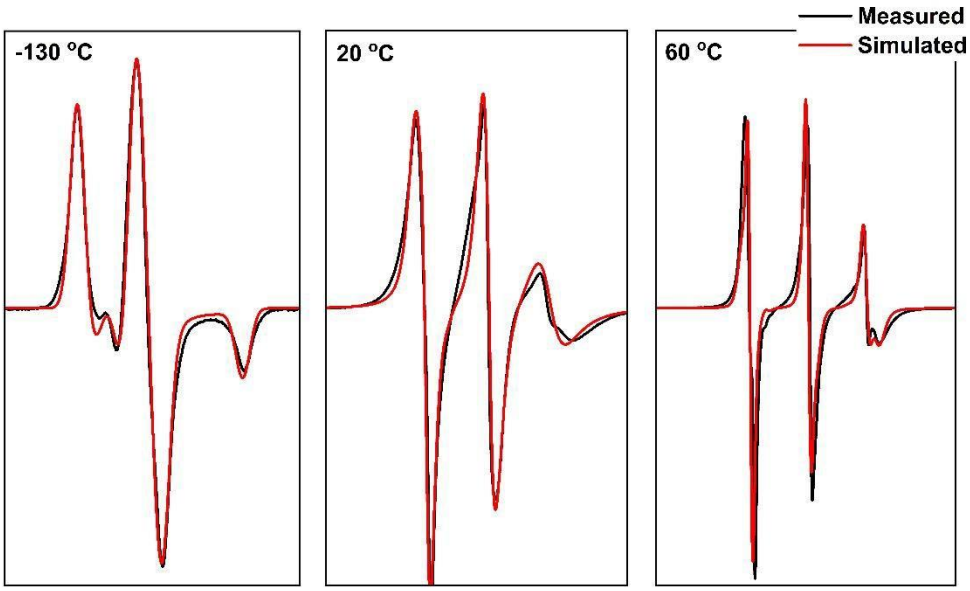

Figure S14. Measured (black) and simulated (red) X-band CW EPR spectra of 1 mM [Ch][TEMPO-COO] in CAGE. The measurements were performed at 100 kHz mod. frequency and 1 mW microwave power.

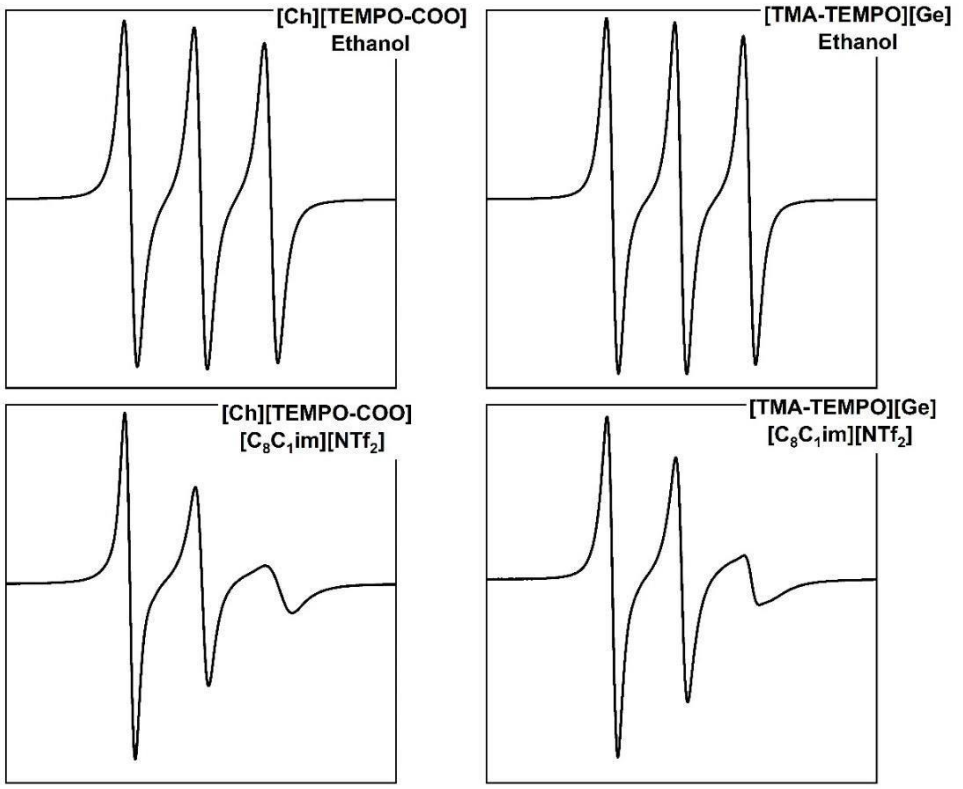

Figure S15. Measured X-band CW EPR spectra of 1 mM [Ch][TEMPO-COO] and [TMA-TEMPO][Ge] in ethanol (top) and $[C_8C_1im][NTf_2]$ ionic liquid. The measurements were performed at 100 kHz mod. frequency and 1 mW microwave power, at 20 °C.

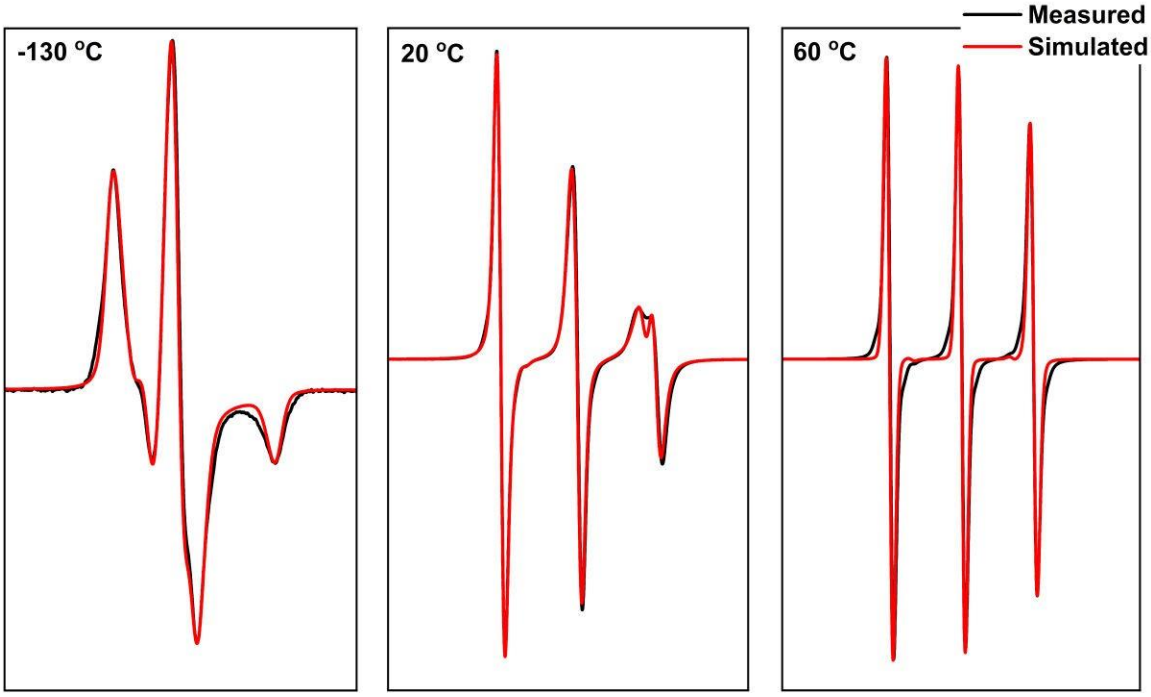

Figure S16. Measured (black) and simulated (red) X-band CW EPR spectra of 1 mM TEMPO in CAOC. The measurements were performed at 100 kHz mod. frequency and 1 mW microwave power.

Table S5. Simulation parameters of the studied radicals in CAGE. *P* is the population of the polar domain and *N* the population of the non-polar domain.

Radical	Solid Phase		Liquid Phase 20 °C		Liquid Phase 60 °C
TEMPO	g_{P1} = [2.0079(4) 2.0070(1) 2.0020(5)] A_P = [0.8 3.1] *lw* = 0.67 P ratio = 0.75	g_{N1} = [2.0100(2) 2.0070(6) 2.0021(2)] A_N = [0.8 3.2] *lw* = 0.6 N ratio = 0.25	g_{N2}=g_{N1} A_N = [0.6 3.49] *lw* = 0.17 τ_c=0.45 ns		g_3=g_{N2} A_3 = [0.6 49] *lw* = 0.17 τ_c=0.06 ns
4-hydroxy-TEMPO	g_{P1} = [2.0077(4) 2.0076(7) 2.0018(7)] A_P = [0.8 3.1] *lw* = 0.8 P ratio = 0.19	g_{N1} = [2.009(1) 2.0058(3) 2.0019(5)] A_N = [0.6 3.32] *lw* = 0.7 N ratio = 0.82	g_{N2}=g_{N1}-0.002 A_P = [0.9 3.1] *lw* = 0.2 τ_c=2.2 ns		g_3=g_{N2} A_3 = [0.85 3.05] *lw* = 0.18 τ_c=0.40 ns
4-oxo-TEMPO	g_{P1} = [2.0078(5) 2.0070(9) 2.0030(3)] A_P = [0.55 3.15] *lw* = 0.78 P ratio = 0.7	g_{N1} = [2.0096(4) 2.0070(5) 2.0015(2)] A_N = [0.4 3.2] *lw* = 0.65 N ratio = 0.3	g_{P2}=g_{P1} A_P = [0.8 2.9] *lw* = 0.15 τ_c=1.6 ns		g_3=g_{P1} A_3 = [0.8 2.9] *lw* = 0.1 τ_c=0.36 ns
[Ch][TEMPO-COO]	g_{P1} = [2.0076(1) 2.0068(5) 2.0021(4)] A_P = [0.73 3.19] *lw* = 0.85 P ratio = 0.26	g_{N1} = [2.0090(9) 2.0061(2) 2.0020(4)] A_N = [0.60 3.32] *lw* = 0.66 N ratio = 0.74	g_{L1}=g_{N1}-0.001 A_P = [0.75 3.2] *lw* = 0.1 τ_c=1.9 ns, ratio = 0.25	g_{L2}=g_{N1}-0.0017 A_N = [0.75 3.3] *lw* = 0.3 τ_c=2.4 ns, ratio = 0.75	Same parameters as 20 °C. Different τ_c and ratios. τ_{c1}=0.5 ns, ratio = 0.45 τ_{c2}=0.6 ns, ratio = 0.55
[TMA-TEMPO][Ge]	g_{P1} = [2.0090(9) 2.0061(1) 2.0021(7)] A_P = [0.65 3.32] *lw* = 0.7 P ratio = 0.8	g_{N1} = [2.0111(6) 2.0046(7) 2.0011(3)] A_N = [0.5 3.34] *lw* = 0.67 N ratio = 0.2	g_{L1}=g_{P1}-0.001 A_P = [0.7 3.1] *lw* = 0.12 τ_c=1.4 ns, P ratio = 0.48	g_{L2}=g_{P1} A_N = [0.9 3.1] *lw* = 0.14 τ_c=4.3 ns, N ratio = 0.52	Same parameters as 20 °C. Different τ_c and ratios. τ_{c1}=0.45 ns, ratio = 0.32 τ_{c2}=2.1 ns, ratio = 0.68

*For the simulation of the spectra. A_{zz} was calculated from the outer extrema of the solid phase. A_{iso} has calculated from the outer extrema of the liquid phases. The *g* values always match the g_{iso} in their corresponding phase. The *A*-vector has been considered axial with $A_{xx} = A_{yy}$, so $A = [A_{xx}\ A_{zz}]$.

Crystal data for **[Ch][TEMPO-COO]**: $C_5H_{14}NO{\cdot}C_{10}H_{17}NO_3{\cdot}1.25(C_2H_6O)$, M = 361.00 g mol^{-1}, orthorhombic, *Pna*2$_1$ (no. 33), a = 15.2287(15), b = 23.0298(18), c = 5.8087(4) Å, V = 2037.2(2) Å^3, Z = 4, D_c = 1.177 g cm^{-3}, μ(Mo-Kα) = 0.085 mm^{-1}, T = 173 K, colourless needles, Agilent Xcalibur 3 E diffractometer; 3016 independent measured reflections (R_{int} = 0.0378), F^2 refinement,[3,4,5] R_1(obs) = 0.0502, wR_2(all) = 0.1067, 1990 independent observed absorption-corrected reflections [$|F_o| > 4\sigma(|F_o|)$, completeness to θ_{full}(25.2°) = 98.7%], 201 parameters. The absolute structure of [Ch][TEMPO-COO] could not be determined [Flack parameter x^+ = –1.5(10)]. **CCDC 2283380**.

The O1–H hydrogen atom in the structure of [Ch][TEMPO-COO] was located from a ΔF map and refined freely subject to an O–H distance constraint of 0.90 Å. The included solvent was found to be highly disordered, and the best approach to handling this diffuse electron density was found to be the SQUEEZE routine of PLATON.[6] This suggested a total of 125 electrons per unit cell, equivalent to 31.3 electrons per asymmetric unit. Before the use of SQUEEZE the solvent most resembled ethanol (C_2H_6O, 26 electrons), and 1.25 ethanol molecules corresponds to 32.5 electrons, so this was used as the solvent present. As a result, the atom list for the asymmetric unit is low by 1.25(C_2H_6O) = $C_{2.5}H_{7.5}O_{1.25}$ (and that for the unit cell low by $C_{10}H_{30}O_5$) compared to what is actually presumed to be present.

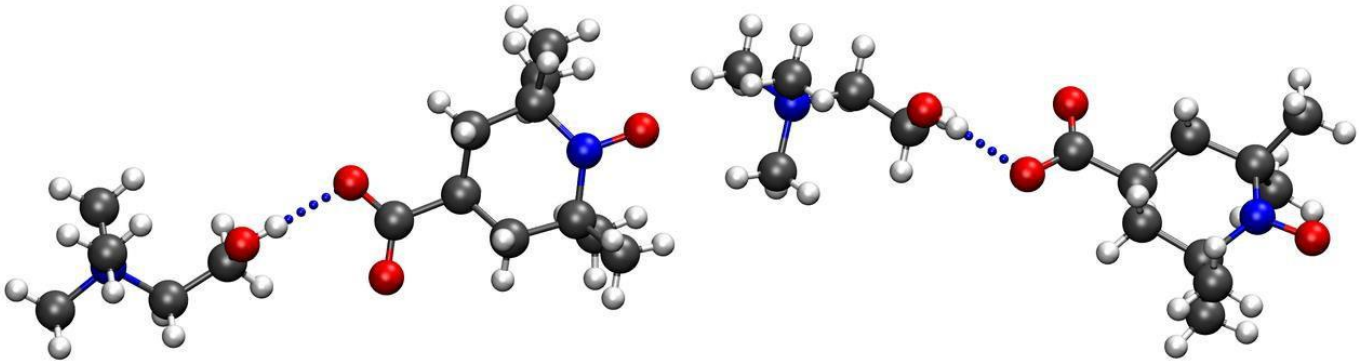

Figure S17. Crystal structure of [Ch][TEMPO-COO] (50% probability ellipsoids) as obtained by single-crystal X-ray crystallography. Two repeating units are shown in this figure. The charged part of the cholinium cation interacts with the N-O radical, while the hydroxyl group hydrogen bonds with the carboxylate anion.

Table S6. Simulation parameters of the studied radicals in CAOC. *P* is the population of the polar domain and *N* the population of the non-polar domain.

Radical	Solid Phase		Liquid-Crystalline Phase		Isotropic Phase
TEMPO	g_{P1} = [2.0079(4) 2.0075(1) 2.0020(5)] A_P = [0.8 3.1] *lw* = 0.72 P ratio = 0.32	g_{N1} = [2.0108(9) 2.0067(6) 2.0025(9)] A_N = [0.6 3.4] *lw* = [0.37 0.3] N ratio = 0.68	$g_{P2}=g_{P1}$ A_P = [0.8 3.3] *lw* = [0.15 0.03] τ_c=0.48 ns, P ratio = 0.48	$g_{N2}=g_{N1}$-0.0003 A_N = [0.6 3.25] *lw* = [0.15 0.03] τ_c=0.52 ns, N ratio = 0.52	$g_3=g_{N1}$-0.0005 A_3 = [0.75 3.3] *lw* = 0.17 τ_c=0.09 ns
4-hydroxy-TEMPO	g_{P1} = [2.0077(4) 2.0076(7) 2.0018(7)] A_P = [0.8 3.1] *lw* = 0.8 P ratio = 0.4	g_{N1} = [2.0105(3) 2.0067(3) 2.0023(5)] A_N = [0.6 3.4] *lw* = 0.5 N ratio = 0.6	$g_{P2}=g_{P1}$ A_P = [0.8 3.3] *lw* = [0.16 0.03] τ_c=0.54 ns, P ratio = 0.58	$g_{N2}=g_{N1}$-0.0001 A_N = [0.6 3.25] *lw* = [0.1 0.13] τ_c=0.54 ns, N ratio = 0.42	$g_3=g_{N1}$-0.00035 A_3 = [0.8 3.3] *lw* = 0.19 τ_c=0.13 ns
4-oxo-TEMPO	g_{P1} = [2.0085(5) 2.0062(5) 2.0020(3)] A_P = [0.5 0.4 3.2] *lw* = 0.68 P ratio = 0.7	g_{N1} = [2.0096(4) 2.0070(5) 2.0015(2)] A_N = [0.4 3.2] *lw* = 0.65 N ratio = 0.3	$g_{P2}=g_{P1}$+0.0002 A_P = [0.32 0.55 3.5] *lw* = 0.094 τ_c=0.58 ns, P ratio = 0.7	$g_{N2}=g_{N1}$-0.0002 A_N = [0.51 3.29] *lw* = 0.08 τ_c=0.42 ns, N ratio = 0.3	$g_3=g_{N1}$+0.00035 A_3 = [0.5 3.45] *lw* = 0.1 τ_c=0.14 ns
[Ch][TEMPO-COO]	g_{P1} = [2.0076(1) 2.0068(5) 2.0021(4)] A_P = [0.73 3.19] *lw* = 0.85 P ratio = 0.66	g_{N1} = [2.0109(9) 2.0073(4) 2.0020(1)] A_N = [0.47 3.56] *lw* = 0.66 N ratio = 0.34	$g_{P2}=g_{P1}$+0.00024 A_P = [0.8 3.36] *lw* = 0.17 τ_c=0.9 ns, P ratio = 0.6	$g_{N2}=g_{N1}$-0.00017 A_N = [0.5 3. 5] *lw* = 0.14 τ_c=0.75 ns, N ratio = 0.4	$g_3=g_{N1}$-0.0007 A_3 = [0.74 3.27] *lw* = 0.15 τ_c=0.34 ns
[TMA-TEMPO][Oc]	g_{P1} = [2.0093(9) 2.0064(8) 2.0036(8)] A_P = [0.73 3.37] *lw* = 0.78 P ratio = 0.6	g_{N1} = [2.0111(6) 2.0046(7) 2.0011(3)] A_N = [0.5 3.34] *lw* = 0.67 N ratio = 0.4	$g_{P2}=g_{P1}$-0.001 A_P = [0.8 3.3] *lw* = 0.2 τ_c=2.5 ns, P ratio = 0.35	$g_{N2}=g_{N1}$+0.001 A_N = [0.5 3.3] *lw* = 0.1 τ_c=3.1 ns, N ratio = 0.65	$g_3=g_{N1}$+0.0005 A_3 = [0.65 3.45] *lw* = 0.15 τ_c=0.6 ns

*For the simulation of the spectra. A_{zz} was calculated from the outer extrema of the solid phase. A_{iso} has calculated from the outer extrema of the liquid phases. The *g* values always match the g_{iso} in their corresponding phase. The *A*-vector has been considered axial with $A_{xx} = A_{yy}$, so $A = [A_{xx}\ A_{zz}]$.

Table S7. Simulation parameters of the studied radicals in BTMAAOC. *P* is the population of the polar domain and *N* the population of the non-polar domain.

Radical	Solid Phase		Liquid-Crystalline Phase		Isotropic Phase
TEMPO	g_{P1} = [2.0077(4) 2.0073(1) 2.0018(5)] A_P = [0.8 3.2] *lw* = 0.7 P ratio = 0.48 Exp. Ordering = −0.35	g_{N1} = [2.0112(9) 2.0071(6) 2.0029(9)] A_N = [0.7 3.38] *lw* = 0.6 N ratio = 0.52 Exp. Ordering = −0.35	$g_{P2}=g_{P1}$+0.0004 A_P = [0.75 3.38] *lw* = [0.15 0.03] τ_c=0.45 ns, P ratio = 0.48	$g_{N2}=g_{N1}$-0.0007 A_N = [0.6 3.25] *lw* = [0.1 0.03] τ_c=0.52 ns, N ratio = 0.52	$g_3=g_{N1}$-0.001 A_3 = [0.75 3.3] *lw* = 0.17 τ_c=0.04 ns
4-Hydroxy-TEMPO	g_{P1} = [2.0073(4) 2.0069(1) 2.0014(5)] A_P = [0.65 3.1] *lw* = 0.7 P ratio = 0.37	g_{N1} = [2.0104(9) 2.0063(6) 2.0021(9)] A_N = [0.6 3.4] *lw* = 0.6 N ratio = 0.63	$g_{P2}=g_{P1}$+0.0004 A_P = [0.8 3.4] *lw* = 0.18 τ_c=1.3 ns, P ratio = 0.53	$g_{N2}=g_{N1}$+0.0001 A_N = [0.69 3.3] *lw* = 0.17 τ_c=1.6 ns, N ratio = 0.47	$g_3=g_{N1}$-0.00035 A_3 = [0.69 3.33] *lw* = 0.17 τ_c=0.29 ns
4-Oxo-TEMPO	g_{P1} = [2.0085(5) 2.0062(5) 2.0020(3)] A_P = [0.5 0.4 3.2] *lw* = 0.68 P ratio = 0.6	g_{N1} = [2.0096(4) 2.0070(5) 2.0015(2)] A_N = [0.4 3.2] *lw* = 0.65 N ratio = 0.4	$g_{P2}=g_{P1}$+0.0002 A_P = [0.32 0.55 3.5] *lw* = 0.094 τ_c=0.55 ns, P ratio = 0.6	$g_{N2}=g_{N1}$-0.0002 A_N = [0.51 3.29] *lw* = 0.08 τ_c=0.86 ns, N ratio = 0.4	$g_3=g_{N1}$+0.00035 A_3 = [0.5 3.45] *lw* = 0.1 τ_c=0.14 ns
[BTMA][TEMPO-COO]	g_{P1} = [2.0076(1) 2.0068(5) 2.0021(4)] A_P = [0.62 3.27] *lw* = 0.7 P ratio = 0.62	g_{N1} = [2.0098(6) 2.0094(8) 2.0026(1)] A_N = [0.6 3.3] *lw* = 0.59 N ratio = 0.38	$g_{P2}=g_{P1}$+0.0003 A_P = [0.8 3.6] *lw* = 0.18 τ_c=1.4 ns, P ratio = 0.74	$g_{N2}=g_{N1}$ A_N = [0.6 3.1] *lw* = 0.2 τ_c=1.7 ns, N ratio = 0.26	$g_3=g_{N1}$-0.0012 A_3 = [0.8 3.2] *lw* = 0.17 τ_c=0.85 ns
[TMA-TEMPO][Oc]	g_{P1} = [2.0093(9) 2.0064(8) 2.0036(8)] A_P = [0.72 3.37] *lw* = 0.75 P ratio = 0.58	g_{N1} = [2.0111(6) 2.0046(7) 2.0011(3)] A_N = [0.5 3.34] *lw* = 0.65 N ratio = 0.42	$g_{P2}=g_{P1}$-0.001 A_P = [0.85 3.3] *lw* = 0.25 τ_c=2.5 ns, P ratio = 0.3	$g_{N2}=g_{N1}$+0.0007 A_N = [0.6 3.4] *lw* = 0.1 τ_c=3.1 ns, N ratio = 0.7	$g_3=g_{N1}$+0.0005 A_3 = [0.65 3.45] *lw* = 0.17 τ_c=0.7 ns

*For the simulation of the spectra. A_{zz} was calculated from the outer extrema of the solid phase. A_{iso} has calculated from the outer extrema of the liquid phases. The *g* values always match the g_{iso} in their corresponding phase. The *A*-vector has been considered axial with $A_{xx} = A_{yy}$, so $A = [A_{xx}\ A_{zz}]$.

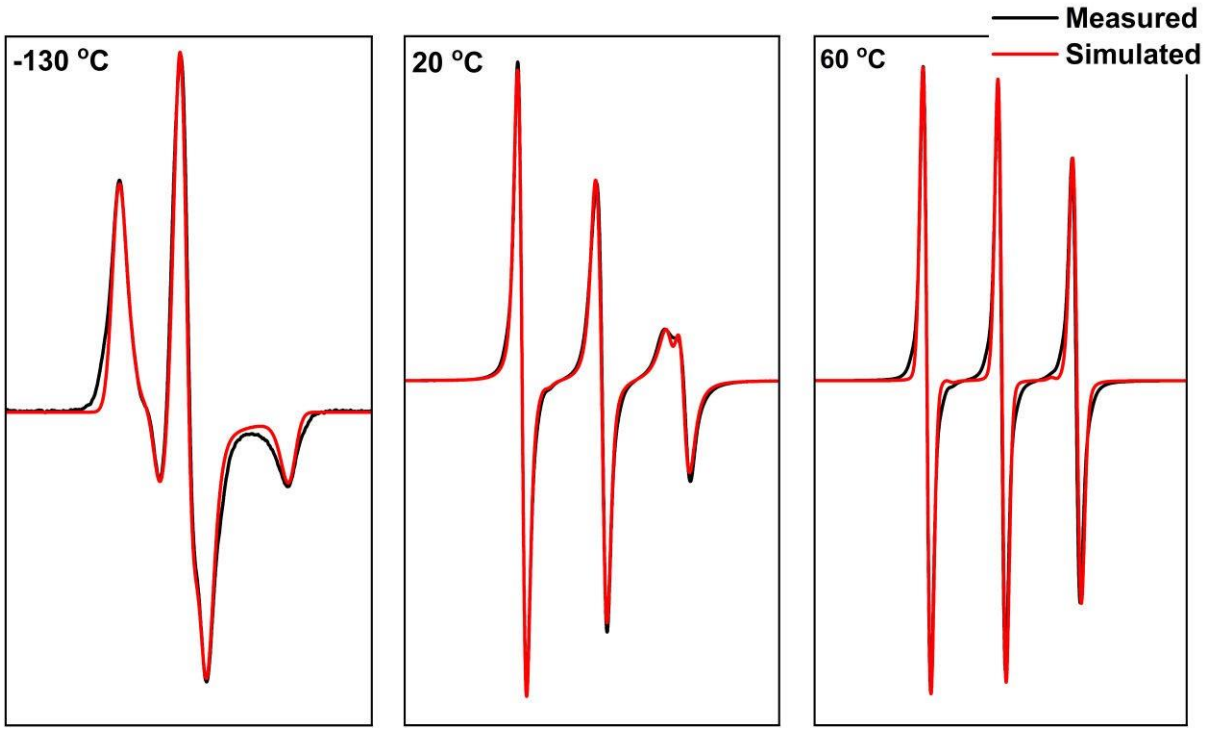

Figure S18. Measured (black) and simulated (red) X-band CW EPR spectra of 1 mM 4-hydroxy-TEMPO in CAOC. The measurements were performed at 100 kHz mod. frequency and 1 mW microwave power.

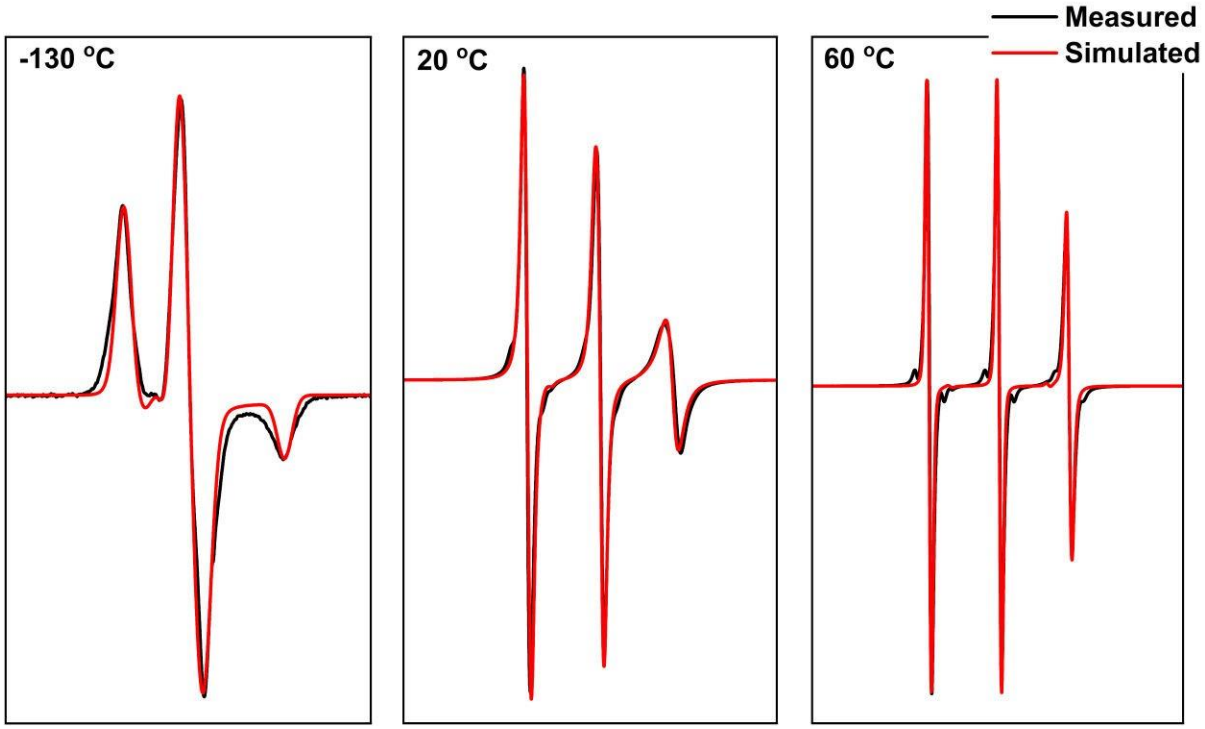

Figure S19. Measured (black) and simulated (red) X-band CW EPR spectra of 1 mM 4-oxo-TEMPO in CAOC. The measurements were performed at 100 kHz mod. frequency and 1 mW microwave power.

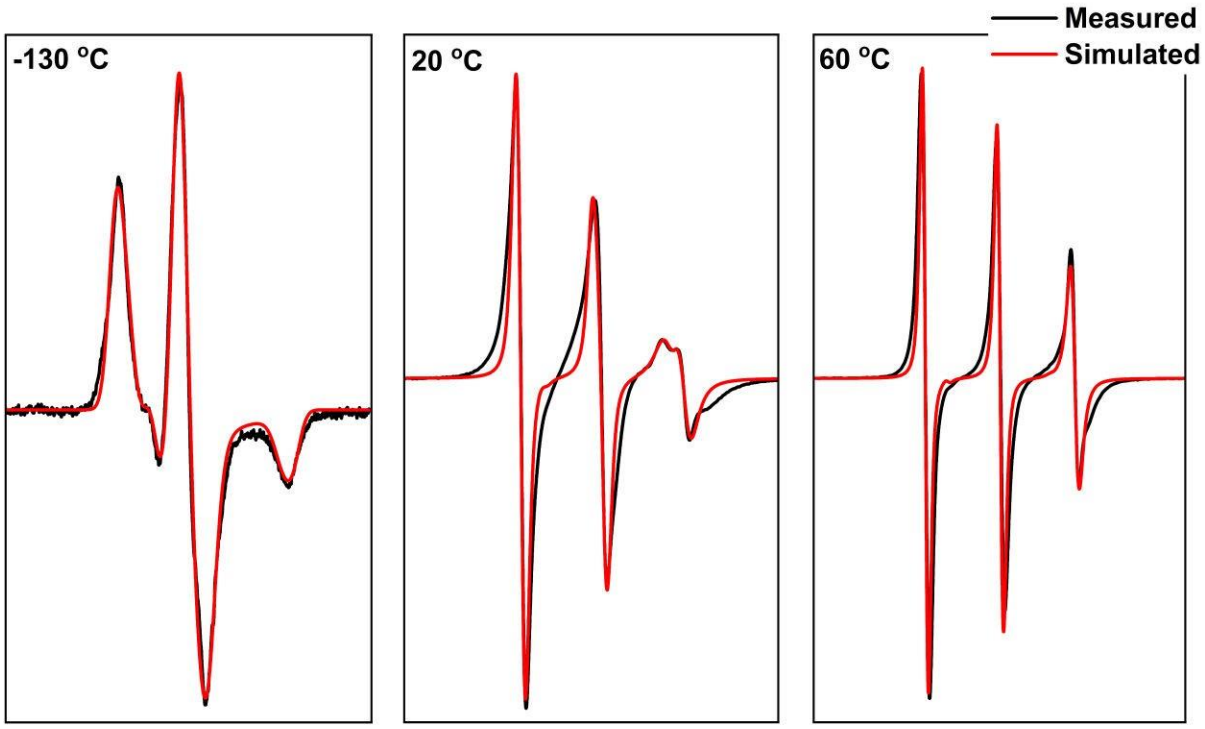

Figure S20. Measured (black) and simulated (red) X-band CW EPR spectra of 1 mM [Ch][TEMPO-COO] in CAOC. The measurements were performed at 100 kHz mod. frequency and 1 mW microwave power.

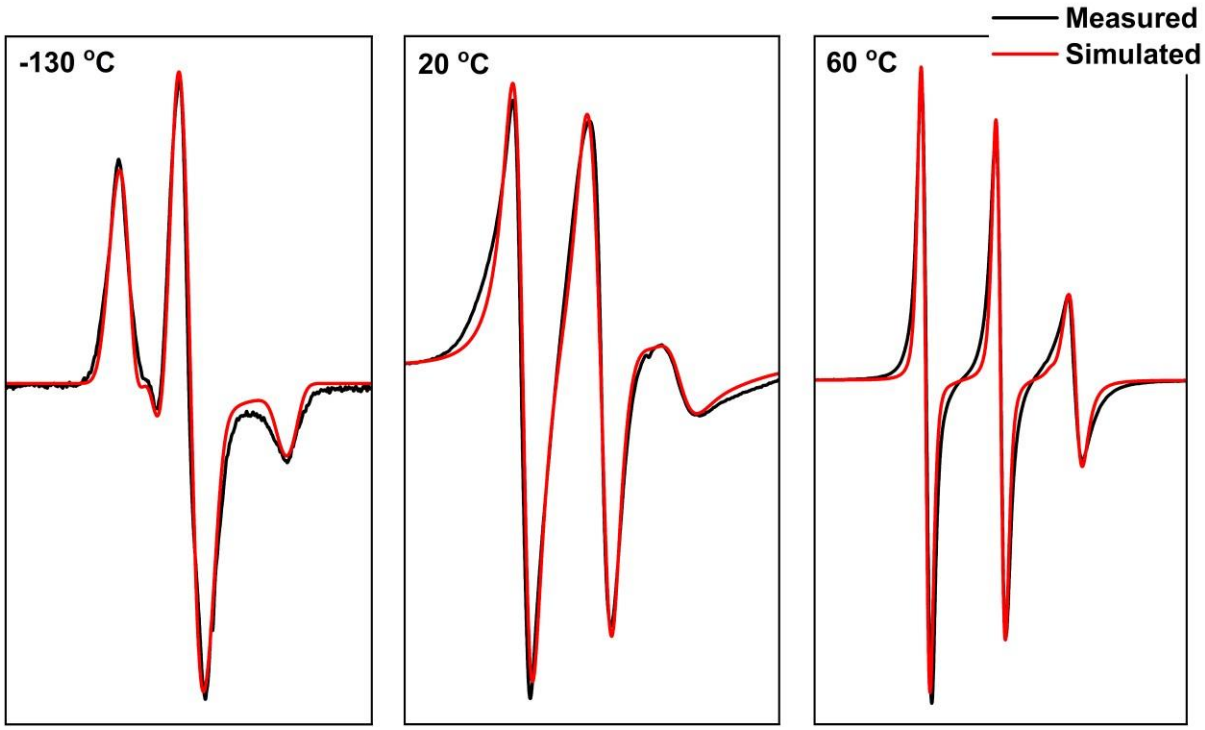

Figure S21. Measured (black) and simulated (red) X-band CW EPR spectra of 1 mM [TMA-TEMPO][Oc] in CAOC. The measurements were performed at 100 kHz mod. frequency and 1 mW microwave power.

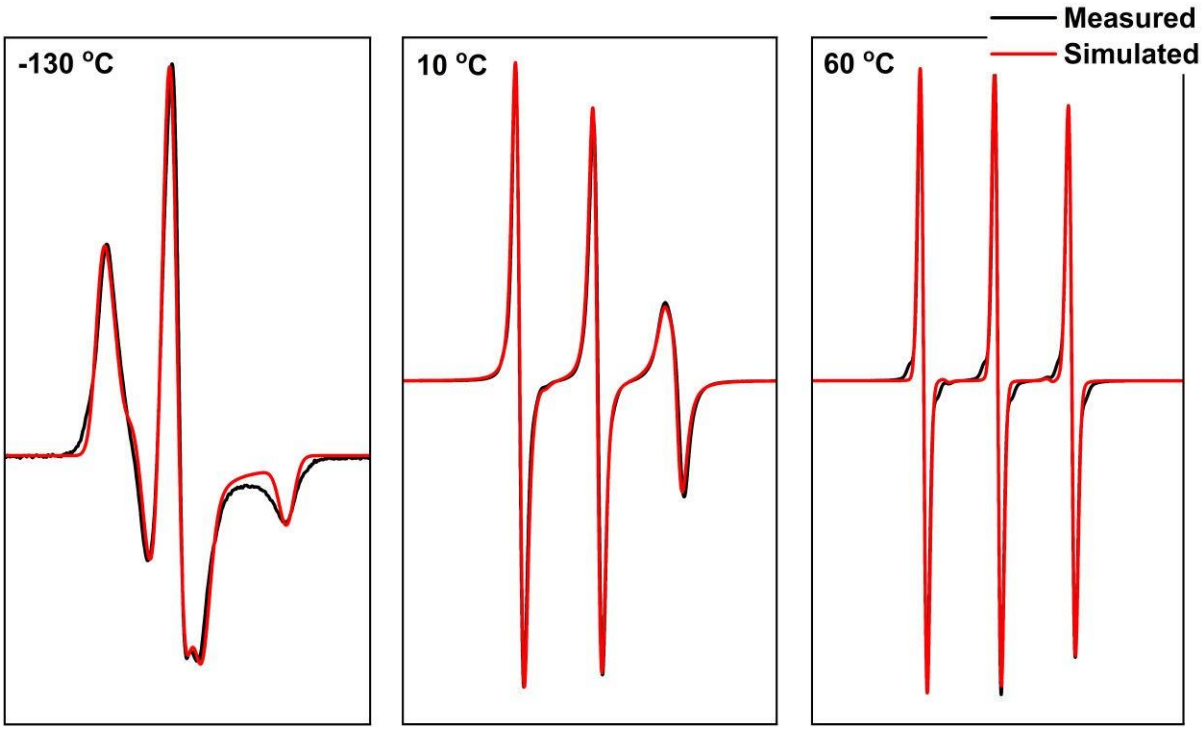

Figure S22. Measured (black) and simulated (red) X-band CW EPR spectra of 1 mM TEMPO in BTMAAOC. The measurements were performed at 100 kHz mod. frequency and 1 mW microwave power.

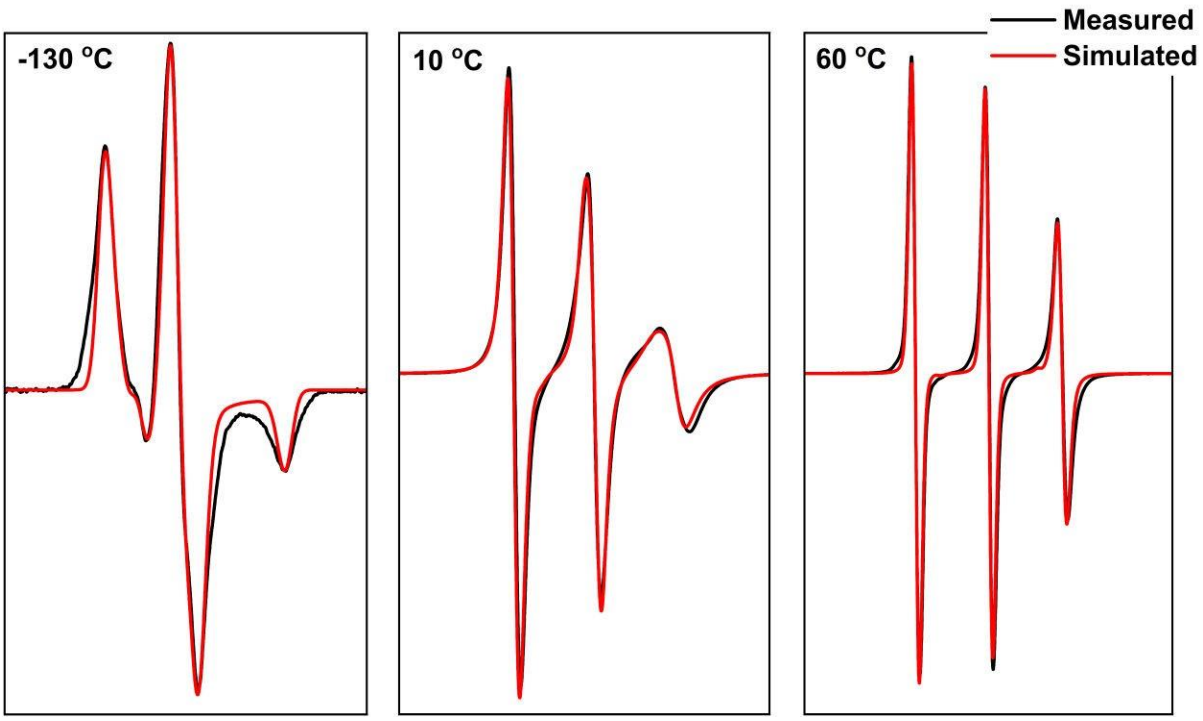

Figure S23. Measured (black) and simulated (red) X-band CW EPR spectra of 1 mM 4-hydroxy-TEMPO in BTMAAOC. The measurements were performed at 100 kHz mod. frequency and 1 mW microwave power.

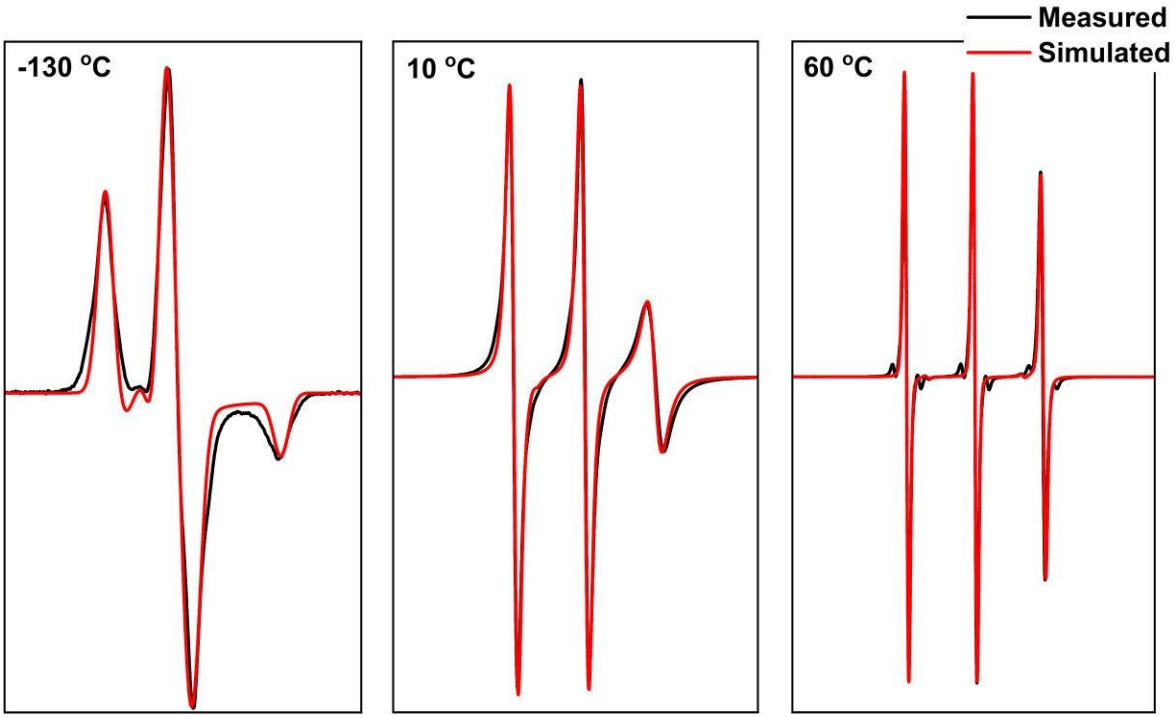

Figure S24. Measured (black) and simulated (red) X-band CW EPR spectra of 1 mM 4-oxo-TEMPO in BTMAAOC. The measurements were performed at 100 kHz mod. frequency and 1 mW microwave power.

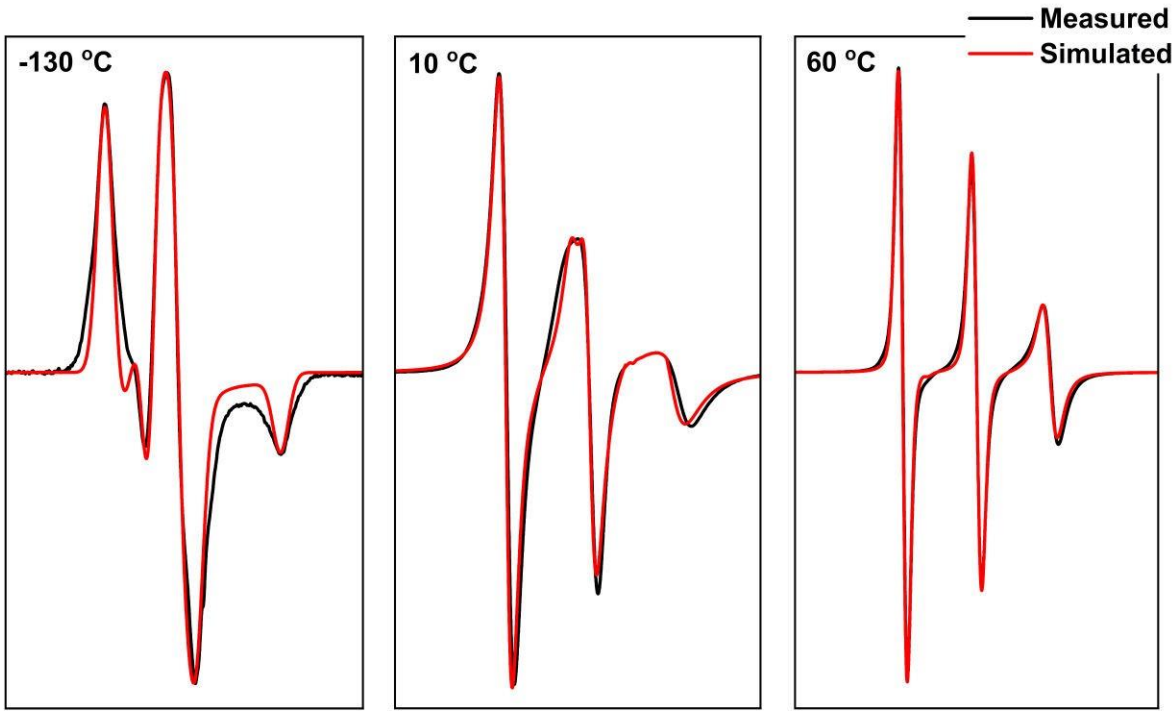

Figure S25. Measured (black) and simulated (red) X-band CW EPR spectra of 1 mM [Ch][TEMPO-COO] in BTMAAOC. The measurements were performed at 100 kHz mod. frequency and 1 mW microwave power.

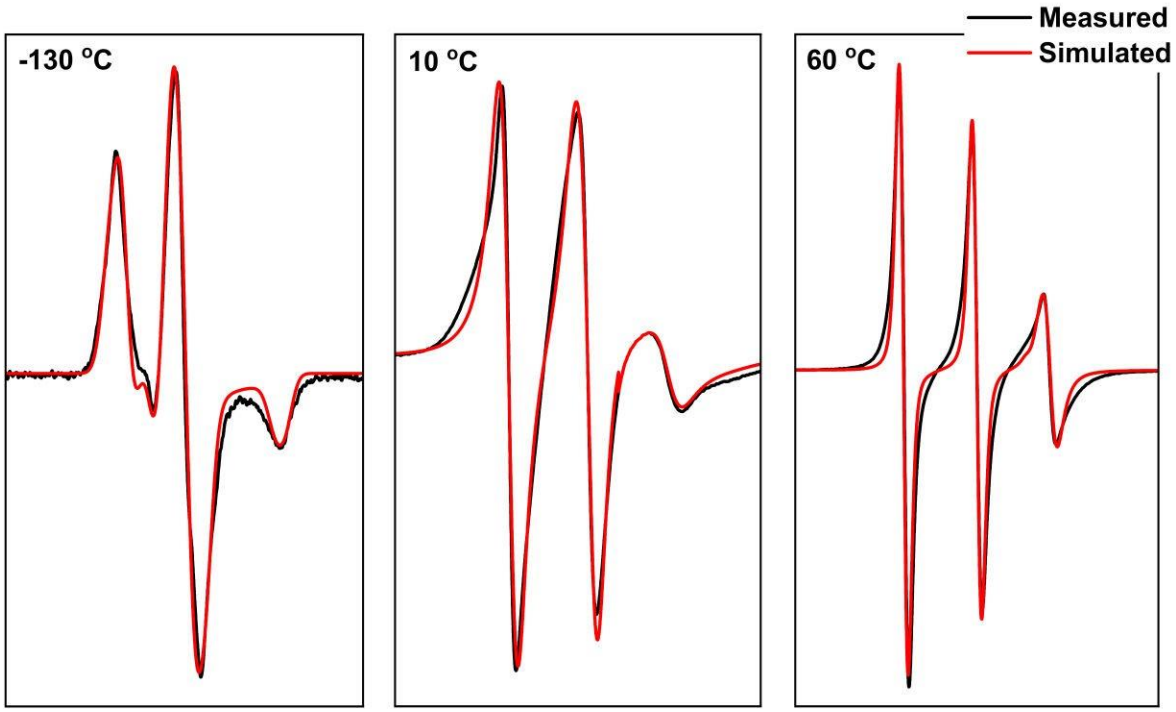

Figure S26. Measured (black) and simulated (red) X-band CW EPR spectra of 1 mM [TMA-TEMPO][Oc] in BTMAAOC. The measurements were performed at 100 kHz mod. frequency and 1 mW microwave power.

G. References

1 M. Zakrewsky, K. S. Lovejoy, T. L. Kern, T. E. Miller, V. Le, A. Nagy, A. M. Goumas, R. S. Iyer, R. E. DelSesto, A. T. Koppisch, D. T. Fox and S. Mitragotri, Proc. Natl. Acad. Sci. U. S. A., 2014, 111, 13313–13318.

2 J. Luo, B. Hu, C. Debruler and T. L. Liu, Angew. Chemie Int. Ed., 2018, 57, 231–235.

3 O.V. Dolomanov, L.J. Bourhis, R.J. Gildea, J.A.K. Howard, H. Puschmann, J. Appl. Cryst., 2009, 42, 339-341.

4 SHELXTL v5.1, Bruker AXS, Madison, WI, 1998.

5 SHELX-2013, G.M. Sheldrick, *Acta Cryst.*, 2015, **C71**, 3-8.

6 A.L. Spek (2003, 2009) PLATON, A Multipurpose Crystallographic Tool, Utrecht University, Utrecht, The Netherlands. See also A.L. Spek, *Acta. Cryst.*, 2015, **C71**, 9-18.